October 2024
CERN, CH-1211 Geneva, Switzerland

Gamma Spectroscopy of ^{129m}Xe Samples Produced at the MARIA Reactor for the Gamma-MRI Project

Author: Bethsaida Zamora
Supervisors: Magdalena Kowalska and Mateusz Chojnacki

Keywords: Gamma spectroscopy, Neutron capture cross section, ^{128}Xe, ^{129m}Xe.

Abtract

This report details the gamma spectroscopy analysis of a ^{129m}Xe sample produced through neutron activation of ^{128}Xe at the MARIA reactor. The energy, resolution, and efficiency calibrations of the gamma detector were performed, along with the identification and activity estimation of key radionuclides and external contaminants. Python scripts were developed for each required peak fitting and calibration curve. Special focus was given to the 196.5 keV gamma peak of ^{129m}Xe, due to its importance for the Gamma-MRI project. The activity of ^{129m}Xe was estimated to be 77(4) MBq at the end of irradiation, and with this, the cross-section of the $^{128}Xe(n,\gamma)^{129m}Xe$ reaction was estimated to be 0.31(6) b, consistent with available literature.

Contents

1 Introduction

The Gamma-MRI project aims to develop a clinical molecular imaging device based on the principle of anisotropic gamma emission from hyperpolarized metastable xenon. This revolutionary technology allows the simultaneous exploitation of the sensitivity of gamma ray detection and the spatial resolution of MRI, while operating with a low magnetic field [3].

Due to the interdisciplinary nature of this project, it is being carried out through a multi-institutional collaboration, including ISOLDE, responsible for the production of ^{129m}Xe and ^{131m}Xe isotopes [5, 1].

As part of the summer student program at CERN, my task was to perform a gamma spectroscopy analysis of the ^{129m}Xe samples produced at the MARIA Reactor [6] via neutron activation of a ^{128}Xe-enriched sample, as well as to estimate the cross-section for the $^{128}Xe(n,\gamma)^{129m}Xe$ reaction.

For this purpose, the energy, resolution, and efficiency calibration of the gamma detector was performed. The written Python scripts can be found in the GitHub repositories available in [7]. Subsequently, the main radionuclides present in the sample were identified, and their activities were estimated.

2 Gamma detector calibration

2.1 Calibration and measurement setup

In order to analyze the ^{129m}Xe sample, a gamma spectroscopy study was conducted using a Canberra GX6020 high-purity germanium detector. The different implemented setups used for the calibration of the detector and measurement of the sample are shown in figure 1.

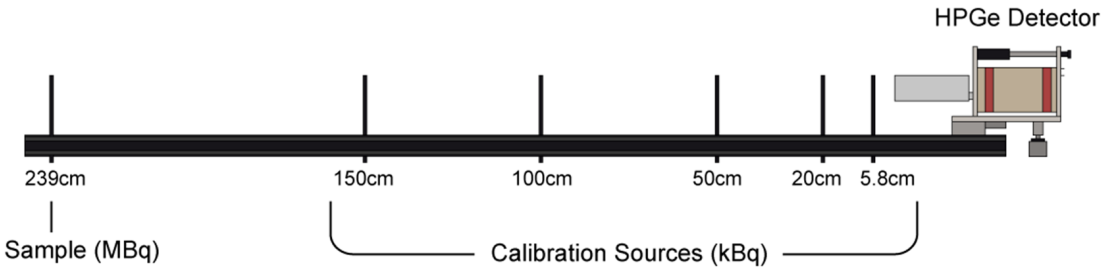

Figure 1: A sketch illustrating the positions where the sample and calibration sources were placed, along with the order of magnitude of their activities

The following subsections display the procedures for the energy, resolution, and efficiency calibration of the gamma detector.

2.2 Energy calibration

Figure 2(a) shows the energy calibration curve, which was obtained using a configuration of 20 *cm* detector-source distance with five different calibration sources: ^{60}Co, ^{137}Cs, ^{152}Eu, ^{133}Ba, and ^{207}Bi, whose gamma emissions range from 53 to 1770 keV.

To include a higher energy range, gamma lines from background radionuclides such as ^{212}Bi, ^{214}Bi, ^{208}Tl, ^{63}Cu, ^{40}K, and ^{228}Ac were taken into account.

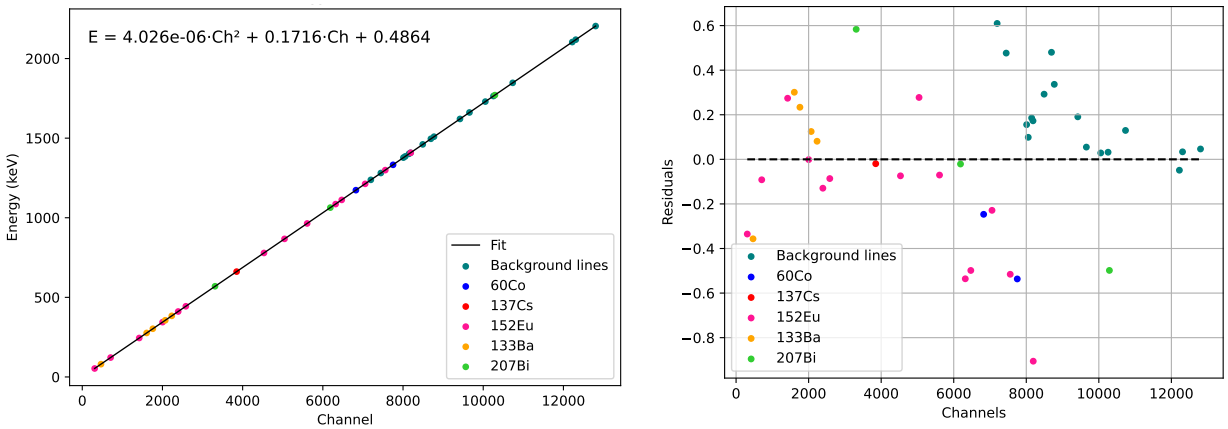

(a) Energy as a function of detector channels (b) Residual plot

Figure 2: The energy calibration curve and its residual analysis.

Even though the curve shown in 2(a) resembles a linear function, a second-order polynomial was used considering the residual analysis, which is shown in 2(b).

2.3 Resolution calibration

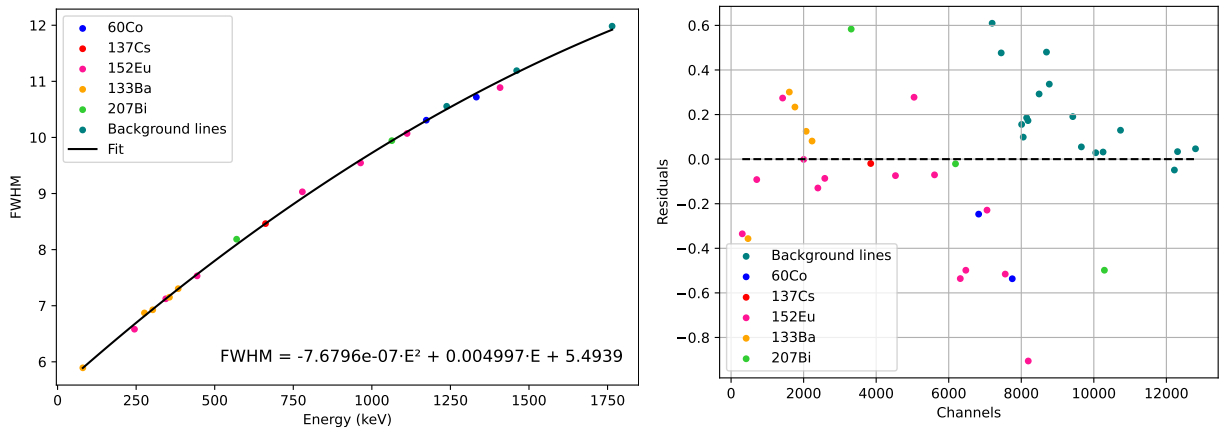

(a) FWHM as a function of energy (b) Residual plot

Figure 3: The resolution calibration curve and its residual analysis.

The full width at half maximum, $FWHM = 2\sqrt{2ln(2)}\sigma$ [2], as a function of the energy, is plotted in figure 3(a) and its corresponding residual plot is shown in 3(b). This calibration was later needed to differentiate peaks generated by more than one energy that are very close in range.

As before, the 20 *cm* detector-source configuration in conjunction with the background peaks corresponding to the radionuclides mentioned in section 2.2, were used. However, in this respect, only statistically significant peaks were used, i.e, peaks formed by more than 10000 counts.

2.4 Efficiency calibration

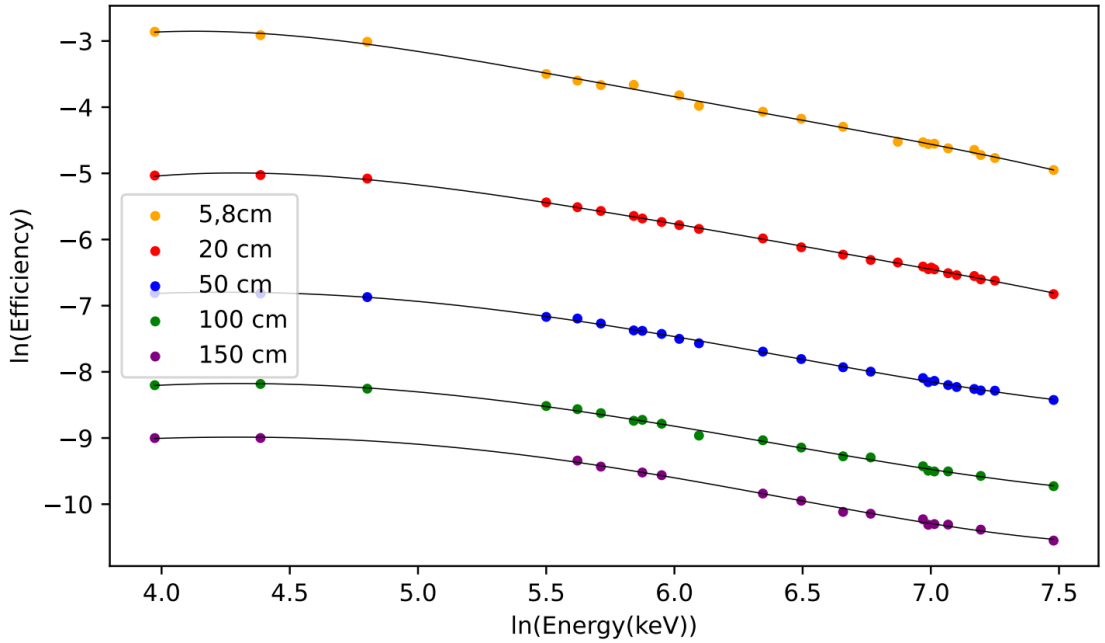

Figure 4: Natural logarithm of efficiency as a function of the natural logarithm of energy for $5.8, 20, 50, 100$, and 150 *cm* detector-source distances.

The detection efficiency is defined by the ratio between the number of counts and the actual number of decays that occurred during the same time [2]. With the number of decays given by $N = A\ t_{live}\ b_r$, where A represents the activity of the calibration source, which was assumed constant, t_{live} is the live time, and b_r is the branching ratio associated with the particular decay.

Due to the large expected activity of the sample, which was on the order of MBq, and the fact that the activity of the available calibration sources was on the order of kBq, placing them both in the same position was not feasible. For this reason, it was decided to place the calibration sources at distances of 5.8, 20, 50, 100, and 150 *cm*.

Figure 4 shows the first efficiency calibration curve for the specified detector-source distances. This approach allows for the later estimation of the efficiency for any given distance, as long as it is reasonably not too far from the calibration points.

3 Estimation of the ^{129m}Xe activity

Among all the peaks found in the sample, there is particular interest in the 196.5 keV peak which is the gamma decay of interest of ^{129m}Xe for the Gamma-MRI project.

As shown in figure 1, the sample was placed 239 cm away from the detector, for this reason the efficiency for each particular energy was rescaled for the actual configuration using the following equation:

$$\frac{eff_x}{eff_{20cm}} = \frac{A}{(B+x)^2},$$

where, for a given energy, $\frac{eff_x}{eff_{20cm}}$ is the ratio between the efficiency at a certain distance x and the efficiency at 20 cm detector-source distance, meanwhile A and B are constants to be determined. However, one expects A to approach $(20\ cm + B)^2$, since the chosen fitting function is based on the principle that the geometrical detection efficiency is inversely proportional to the square of the detector-source distance.

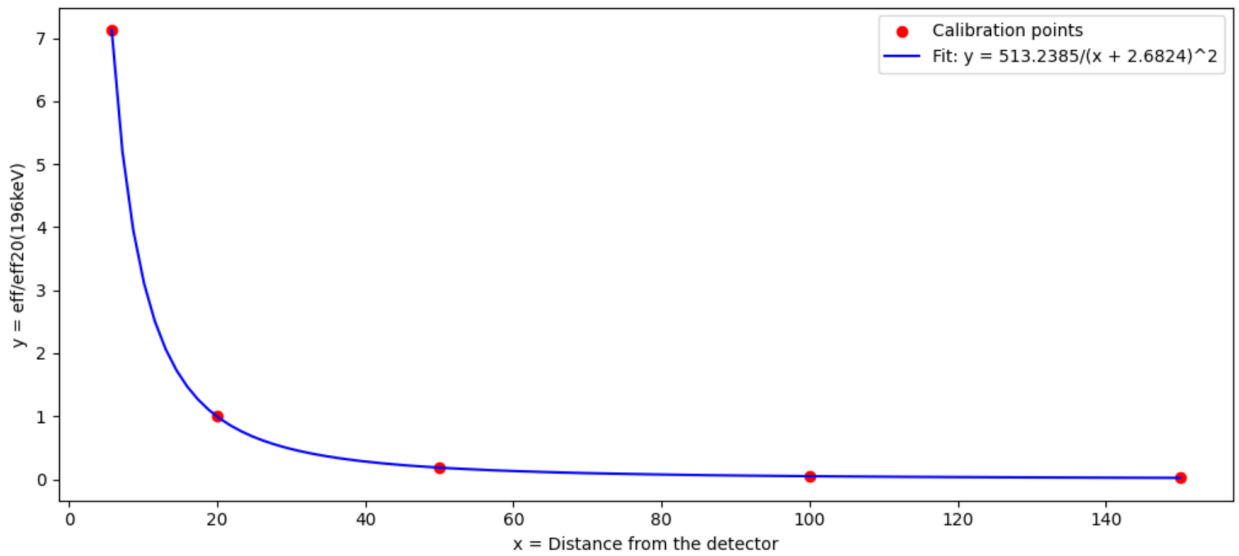

Figure 5: $\frac{eff}{eff_{20cm}}$ as a function of distance from the detector for $E = 196.5\ keV$

The normalized efficiency as a function of distance for this energy configuration is shown in figure 5, and the fitting parameters were found to be $B = 2.68(4)\ cm$ and $A = 513(4)\ cm^2$ for an efficiency of $4.31 \times 10^{-5}(7)$ for the 239 cm detector-sample configuration. Hence, the

activity of ^{129m}Xe at the beginning of the measurement was estimated to be 55(2) MBq, which will be used in the following section to estimate the cross-section of $^{128}Xe(n,\gamma)^{129m}Xe$.

The previous procedure was applied for each peak of interest in order to estimate the efficiency corresponding to its energy. In other words, a fitting curve as shown in figure 5 was generated for each energy E.

4 Estimation of the cross-section of the $^{128}Xe(n,\gamma)^{129m}Xe$ reaction

As a verification exercise, the cross-section of the $^{128}Xe(n,\gamma)^{129m}Xe$ reaction was estimated and compared with the available literature. For this reaction, the cross-section is given by

$$\sigma = \frac{A[^{129m}Xe]}{N[^{128}Xe]\phi(1 - exp(-\lambda[^{129m}Xe]t))}.$$

Where the number of ^{128}Xe atoms inside the glass vial was $N[^{128}Xe] = 4.7(5) \times 10^{18}$. The thermal neutron flux at the MARIA reactor was $\phi = 1.1(2) \times 10^{14}\ 1/cm^2s$. The decay constant of ^{129m}Xe is $\lambda = ln(2)/T_{1/2}$, where $T_{1/2} = 8.88(2)\ days$. The irradiation time was $t = 8.68\ days$. And the activity of ^{129m}Xe at the end of the irradiation, $A[^{129m}Xe]$, was estimated to be 77(4) MBq by knowing the time between the end of the irradiation and the beginning of the measurement, which was 4.40(1) $days$, and the activity at the beginning of the measurement, which was indicated in section 2.4.

Finally, the cross-section was estimated to be equal to 0.31(6) b which is with a good agreement with available literature value (Chojnacki, 2024). [1]

5 Determination of the radionuclides present in the ^{129m}Xe sample

The main radionuclides present in the sample were manually identified with the use of IAEA's nuclear structure and decay data searching tool [4]. Figure 6 shows both the sample and the background spectra normalized to the live time of sample measurement. The figure also includes labels identifying the peaks corresponding to the detected radionuclides.

Among the detected radionuclides there are:

- ^{129m}Xe, ^{127}Xe and ^{125}Xe are known to come from the gas contained inside the vial, which prior to the irradiation, consisted of highly enriched (99.3%) ^{128}Xe and ($< 0.7\%$) $^{124,126,129,130,131,132,134,136}Xe$.

- ^{125}I and ^{126}I also originate from the gas. Since the identification was done for energies above 100 keV, ^{125}I ($T_{1/2} = 59.4\ days$) was not directly detected, however, it is known

to be present in the gas due to the presence of its parent, ^{125}Xe, and because it undergoes neutron capture to form ^{126}I.

- ^{24}Na and ^{42}K are due to the neutron capture reaction experimented by the ^{23}Na and ^{41}K contained in the glass.
- In contrast, radionuclides such as ^{99}Mo, ^{99m}Tc, ^{82}Br, ^{46}Sc, ^{51}Cr, ^{140}La, ^{187}W, ^{56}Fe ^{76}As, and ^{86}Rb are believed to be external contaminants resulting from the handling of the glass vial inside the reactor.

Subsequently, the activities of the found radionuclides were estimated. Except for ^{129m}Xe and ^{24}Na, all the activities lay in the range of $1 - 35\ kBq$ four days after the end of irradiation, meanwhile the activity of ^{24}Na was estimated to be $31(1) \times 10^1\ kBq$ at this time.

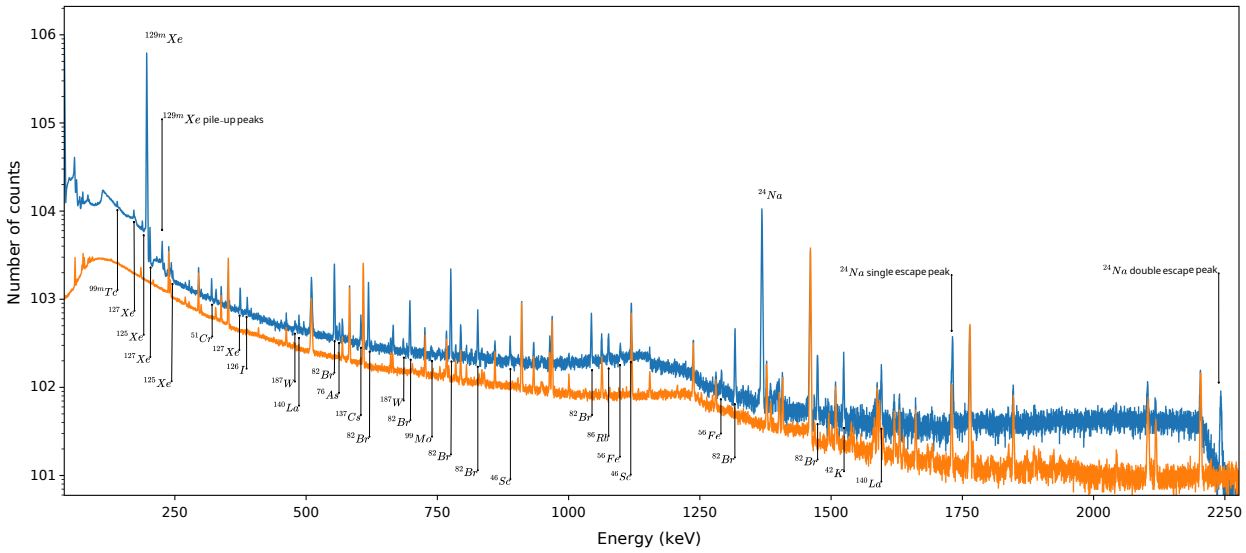

Figure 6: The gamma spectrum of the ^{129m}Xe sample is plotted in blue, while the background spectrum is plotted in orange.

6 Conclusions

- Python scripts were written to fit Gaussian curves and perform the energy, resolution, and efficiency calibration.
- The gamma-emitting radionuclides present in the sample were identified and their activities estimated.
- The cross-section of the neutron capture reaction $^{128}Xe(n,\gamma)^{129m}Xe$ was estimated and compared with literature.

References

[1] M. Chojnacki, K. Kulesz, I. Michelon, N. Azaryan, E. Barbero, B. Crepieux, R. Lica, Ł. Murawski, M. Ziemba, M. Piersa-Siłkowska, K. Vitulova, A. Korgul, R.B. Jolivet, R. Prokopowicz, U. Köster, and M. Kowalska. Production of ^{129m}Xe and ^{131m}Xe via neutron activation of ^{128}Xe and ^{130}Xe at ILL-RHF and NCBJ-MARIA high-flux reactors. *Applied Radiation and Isotopes*, 205:111174, 2024.

[2] K. Debertin and R.G. Helmer. *Gamma- and X-ray spectrometry with semiconductor detectors*. Elsevier Science, 1988.

[3] Gamma MRI. The future of molecular imaging. https://gamma-mri.eu/.

[4] IAEA. Nuclear structure and decay data. https://www-nds.iaea.org/relnsd/NdsEnsdf/QueryForm.html.

[5] ISOLDE. The ISOLDE facility. https://isolde.cern/isolde-facility.

[6] NCBJ. MARIA Research Reactor. https://www.ncbj.gov.pl/en/maria-reactor.

[7] B. Zamora. GitHub repositories. https://github.com/Bethsaida1.